communications biology

A Nature Portfolio journal

Article

https://doi.org/10.1038/s42003-025-08628-1

Macrophagic Ym1 orchestrates γδT cell-derived IL-17 production and keratinocyte functionality to mediate psoriasis-like skin inflammation

Wentao Zhang[1,2,3,8], Fei Li[4,8], Yu Wang[2], Meiyang Fan[2], Yan Zhao[4], Yanglong Guan[2], Yan Zhou[4] ✉, Shemin Lu[1,2,5], Rikard Holmdahl[1,6,7], Liesu Meng[1,2,5] ✉ & Wenhua Zhu[1,2] ✉

Psoriasis is a chronic inflammatory skin disease, with the IL-17 pathway being a key contributor. Ym1, a positionally cloned inflammation regulatory gene linked to various disorders, has an unclear effect on skin inflammation. In this study, the role of Ym1 was investigated in both mannan and imiquimod-induced psoriasis-like dermatitis models, using Ym1-deficient congenic mice. Natural polymorphism of Ym1 influenced the development of skin inflammation, dependent on macrophages, since adoptive transferring of Ym1-deficient macrophages alleviated disease, whereas recombinant Ym1 worsened it. Particularly, Ym1 congenic mice exhibited decreased IL-17 production in innate immune cells, and depletion of γδT cells mitigated disease and lowered skin IL-17 levels. Additionally, RNA-seq analysis revealed Ym1-regulated keratinization in lesional skin. Recombination Ym1 directly influenced the inflammatory response and proliferation of mouse primary keratinocytes. Collectively, we conclude that Ym1 regulates γδT cell-derived IL-17 production and keratinocyte functionality, and thereby contributes to skin inflammation in mice.

Psoriasis, a chronic skin condition characterized by inflammation, exhibits a prevalence ranging from 0.1 to 8% across different geographical regions, impacting over 125 million individuals globally[1,2]. It is characterized by the activation of inflammatory pathways in both the innate and adaptive immune cells triggering the uncontrolled proliferation of keratinocytes (KCs), acanthosis, neovascularization, and significant immune cell infiltration into the skin. The predominant form of this disease, plaque psoriasis (also known as psoriasis vulgaris), comprises over 80% of all cases[1].

As a complex disease, psoriasis is orchestrated by a multifaceted interplay of genetic predispositions, environmental triggers, and immune modulation, all serving as etiological factors. This intricate interplay gives rise to clinical heterogeneity among patients, manifesting in variations such as distinct clinical presentations and differential responses to therapeutic interventions[3]. Previous genetic linkage studies have identified several psoriasis susceptibility (*PSORS*) loci, and among them, HLA-Cw6 is one of the most strongly associated psoriasis susceptibility alleles[4]. Despite the discovery of 63 psoriasis susceptibility loci through advancements in new technologies such as genome-wide association studies, only a small number of these genomic segments highlight a single gene[5]. Therefore, the ongoing exploration of disease susceptibility loci and genes remains a formidable task.

We have previously positionally identified polymorphism within *Chil3*, a gene coding chitinase-like protein 3 (also known as Ym1), as an immune regulator using arthritis mouse model. Both the wild mouse population, and inbred strains, vary in the numbers of functional copies of the *Chil3* gene, having a profound impact on susceptibility to inflammatory

[1]National-local Joint Engineering Research Center of Biodiagnostics and Biotherapy, The Second Affiliated Hospital of Xi'an Jiaotong University, Xi'an, Shaanxi, China. [2]Institute of Molecular and Translational Medicine (IMTM), and Department of Biochemistry and Molecular Biology, Xi'an Jiaotong University Health Science Center, Xi'an, Shaanxi, China. [3]Center of Experiment Teaching for Medical Postgraduates, Xi'an Jiaotong University Health Science Center, Xi'an, Shaanxi, China. [4]Department of Dermatology, The First Affiliated Hospital of Xi'an Jiaotong University, Xi'an, Shaanxi, China. [5]Key Laboratory of Environment and Genes Related to Diseases (Xi'an Jiaotong University), Ministry of Education, Xi'an, Shaanxi, China. [6]Key Laboratory of Surgical Critical Care and Life Support (Xi'an Jiaotong University), Ministry of Education, Xi'an, Shaanxi, China. [7]Section for Medical Inflammation Research, Department of Medical Biochemistry and Biophysics, Karolinska Institute, Stockholm, Sweden. [8]These authors contributed equally: Wentao Zhang, Fei Li. ✉e-mail: yanzhou7798@xjtu.edu.cn; mengliesu@xjtu.edu.cn; zhuwenhua@xjtu.edu.cn

diseases, such as pulmonary inflammation and skin inflammation[6]. Of particular note, we have discovered a new mouse model of skin inflammation, mannan-induced psoriasis-like dermatitis and arthritis (MIP), which can simulate the phenotype of human diseases in many aspects by intranasally or intraperitoneally administering mannan, a *Saccharomyces cerevisiae* cell wall component[6–8]. The Ym1 congenic mice, which carry a naturally occurring haplotype (the RIII haplotype identified from RIIIS/J strain) resulting in deficient production of the Ym1 protein due to *Chil3* polymorphism, exhibit a significant reduction in MIP severity[6]. It highlights the role of Ym1 in mouse psoriasis-like skin inflammation, and understanding its mechanism will help us further explore the role and mechanism of human chitinase-like proteins (CLPs) in psoriasis.

Ym1 is a rodent-specific CLP, lacking chitinase activity, however, it shares significant structural similarity to family 18 chitinases[9]. This suggests a possibility that there exist functionally homologous molecules in human CLPs that exert inflammation regulatory functions similar to Ym1, thereby participating in human diseases. Ym1 has been reported to be associated with host defense for infection[10–12], tissue injury[13], as well as different inflammatory disorders studied using mouse models, including allergic lung inflammation[14,15], EAE[16], atherosclerosis[17,18] and obesity[19]. However, up to now, there is still a lack of in-depth research on the role of Ym1 in the pathogenesis of skin inflammation. The pathogenesis of psoriasis encompasses intricate interactions among KCs, immune cells, and various other skin-resident cells, with the pivotal pathogenic IL-23/IL-17 axis emerging as a crucial player in this inflammatory skin condition[20,21]. Interestingly, although lacking a direct link with psoriasis-like skin inflammation, Ym1 has been found to be closely related to the regulation of IL-17 in mice, since it has been reported that Ym1 could induce the accumulation of neutrophils through the expansion of γδT cell populations that produced IL-17[10].

Therefore, in this study, we have uncovered the crucial function of Ym1 by employing a congenic C57BL/10 mouse strain, expressing a psoriasis susceptible non-classical MHC type I haplotype, the Qa^r allele[22], but also a *Chil3* haplotype derived from the RIIIS/J strain (designated as the RIII haplotype) which results in the natural absence of Ym1 expression, to establish psoriasis models. Our findings demonstrate that Ym1, which is secreted by macrophages, plays a pivotal role in the development of the disease. Specifically, Ym1 leads to an imbalance in skin immune homeostasis, partly by regulating the IL-17-producing cells such as γδT cells. Furthermore, Ym1 could directly target KCs to regulate cell functionality, and thereby contributing to skin inflammation. This would be beneficial for further understanding the immune regulatory role of Ym1 and exploring the relationship between human CLPs and psoriasis in the future.

Results

Natural polymorphism of Ym1 regulates the development of mannan-induced psoriasis-like dermatitis in mice dependent on macrophages

To fully study the role of Ym1 in skin inflammation we induced signs of psoriasis in Ym1 congenic mice (BR.Ncf1*.Ym1$^{\Delta}$) with an RIII haplotype leading to Ym1 deficiency, and their littermate controls (BR.Ncf1*) with a fully Ym1 functional B haplotype (common in C57BL strains), by a single intraperitoneal injection of mannan (Fig. 1a). In line with our previous findings, decreased psoriatic lesions of mouse paws and ears were scored in Ym1 congenic mice, along with the reduction of arthritis symptoms, compared with BR.Ncf1* mice (Fig. 1b). Pathologically, the ear tissues showed reduced epidermal thickness and Munro's microabscesses in Ym1 congenic mice (Fig. 1c).

Then we analyzed the immune regulation in skin and draining lymph nodes of skin and paws, including inguinal lymph nodes and popliteal lymph nodes by flow cytometry, in both strains during the development of MIP. It was interesting that in skin tissue, macrophages were one of the earliest and most significant cell populations to respond to Ym1 regulation, and showed differences on the third and seventh day after mannan treatment (Fig. 1d). At the same time, $CD45^+$ immune cells and/or various subtypes in lymph nodes showed significant decrease in numbers in Ym1 congenic mice compared to BR.Ncf1* control mice, during the onset (D3) or development (D5) of the disease, indicating that Ym1 induces systemic immune regulation in immune organs (Supplementary Fig. 1a, b).

Macrophages are the major source of Ym1, and macrophage infiltration is a common feature of psoriasis and is believed to promote psoriasiform dermatitis[23]. Due to the unique changes of macrophages in the early stages of disease, we focused on their role in Ym1 regulating disease. After intraperitoneal injection of mannan, we found a lower proportion of macrophages among peritoneal exudate cells in Ym1 congenic mice compared to BR.Ncf1* controls (Fig. 1e). We then depleted macrophages by administrating clodronate liposome intraperitoneally in BR.Ncf1* mice (recipient), and cultured bone marrow derived macrophages (BMDM) from BR.Ncf1* and BR.Ncf1*.Ym1$^{\Delta}$ mice respectively. After transplanting these Ym1-sufficient and deficient macrophages, recipient mice were injected with mannan (Fig. 1f). Mice receiving Ym1-deficient macrophages showed less severe skin lesions and arthritis (Fig. 1g).

To further investigate the pathogenic role of Ym1 per se, recombinant Ym1 (rYm1) protein was used as an exogenous supplement. Mice were topically treated with mannan on ear skin to induce inflammation, and rYm1 was intradermally injected to one side of ears and PBS to the other side as control (Fig. 1h). Mice with higher levels of Ym1 protein locally showed stronger skin lesions compared to controls (Fig. 1i, j). The above results show the importance of natural selected polymorphism of Ym1 in mice with skin inflammation, and demonstrate its regulatory role through macrophages.

Macrophage Ym1 tilts skin immune homeostasis in imiquimod-induced psoriasis-like dermatitis

To validate the findings, we used the imiquimod (IMQ)-induced psoriasis-like dermatitis model to induce local skin inflammation (Fig. 2a). The severity of symptoms was evaluated from the erythema, scaling and thickening of skin using a PSI scoring system, and Ym1 congenic mice showed decreased skin scaling (Fig. 2b) and epidermal thickness (Fig. 2c).

Then the immune phenotype was determined by analyzing the immune cell population in skin and draining lymph node by flow cytometry during IMQ-induced psoriasis-like dermatitis. In the skin, the proportions of macrophages and γδT cells were decreased at D5, and neutrophils were later subsequently reduced at D7, in Ym1 congenic mice compared to BR.Ncf1* controls (Fig. 2d). In line with the MIP model, $CD45^+$ immune cells and various subtypes in lymph nodes were all decreased in numbers in Ym1 congenic mice compared to BR.Ncf1* control mice in inguinal lymph nodes (Supplementary Fig. 1c).

Cytokine production is associated with the status of immune regulation, therefore, we analyzed fifteen cytokine expression in skin and serum by using real-time qPCR or Luminex. The expression patterns of cytokines were visualized in heatmaps (Fig. 2e, f). In skin, Ym1 (*Chil3*) mRNA expression was increased in BR.Ncf1* mice in IMQ model, but absent in Ym1-deficient congenic mice (Fig. 2e). Importantly, the mRNA expression of *Il17*, as well as *Il33, Il4, Il13* and *Il10*, were all upregulated in the IMQ group of BR.Ncf1* mice, and downregulated in Ym1 congenic mice (Fig. 2e). Although no statistically significant differences were observed in the mRNA expression levels of *Ifng, Cxcl1, Il25* and *Il5* between the control and IMQ groups in BR.Ncf1* mice, notable differences emerged when comparing the IMQ groups of BR.Ncf1* mice with those of BR.Ncf1*.Ym1$^{\Delta}$ mice (Fig. 2e). In serum, a confirmed decrease was observed in the levels of TNF-α and IL-6 in Ym1 congenic mice, whereas no significant differences were detected for the other cytokines examined (Fig. 2f and Supplementary Fig. 2).

In addition, using two-color immunofluorescence it was found that F4/80^+ macrophages infiltrating into the dermis layer of skin lesions co-expressed Ym1 (Supplementary Fig. 3). Taken together, these results show that Ym1 imbalances skin immune homeostasis of mice, highlighting the role of macrophages in disease, as well as γδT cells.

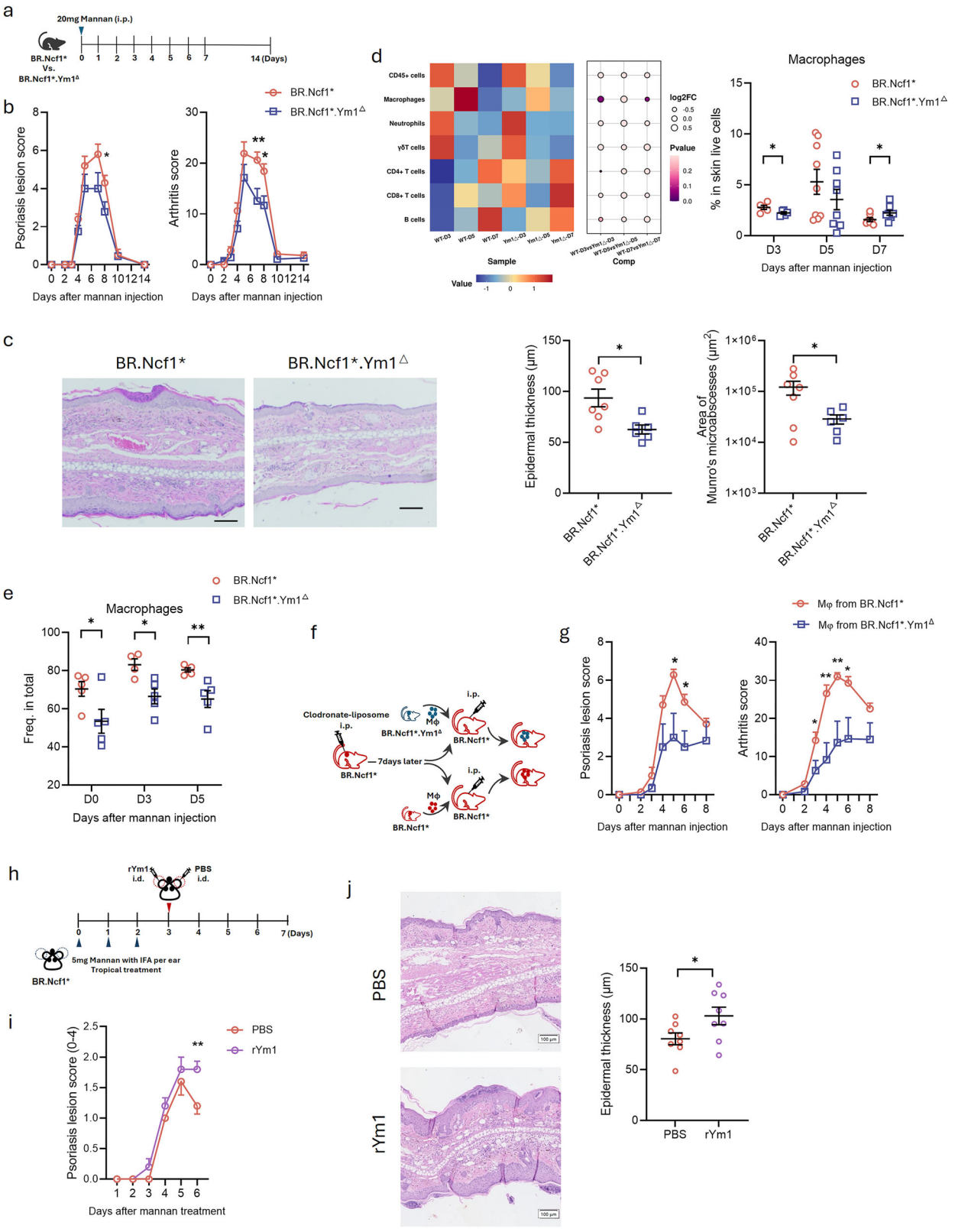

Ym1 regulating IL-17-producing cells contributes to skin inflammation

IL-17 plays a key role in the pathogenesis of psoriasis through its pro-inflammatory and pro-epidermal hyperplasia properties. It is produced by Th17 cells, but also by innate immune cells such as γδT cells, innate lymphocytes type III (ILC3), neutrophils and macrophages[24–27]. To analyze the origin of the relevant IL-17 production in skin of IMQ-induced psoriasis-like dermatitis, flow cytometry was used. Compared to BR.Ncf1* controls, Ym1 congenic mice had less IL-17-producing macrophages and γδT cells (Fig. 3a, b). However, there was no difference in αβT cells, neutrophils, and ILC3 (Fig. 3a, c). The γδT cells are known to be crucial in the IMQ model, producing pro-inflammatory cytokines, such as IL-17, amplify the immune

Fig. 1 | Ym1 regulates the development of mannan-induced psoriasis-like dermatitis in mice dependent on macrophages. a A scheme of mannan-induced psoriasis-like dermatitis using BR.Ncf1* mice and BR.Ncf1*.Ym1$^{\Delta}$ mice. **b** Psoriasis lesion score and arthritis score were assessed. $n = 9–10$. **c** Representative H&E images of skin sections from ears taken on day 7 in mannan-treated mice. Bar = 100 μm. Epidermal thickness and area of Munro's microabscesses were measured. $n = 6–7$. **d** Immune cells of skins from paws taken on day 3, 5 and 7 in mannan-treated mice were analyzed by flow cytometry. Heatmap of all cell populations and histogram of skin macrophages were shown. $n = 5–9$. **e** Macrophages were analyzed in peritoneal exudate cells on day 0, 3 and 5 mannan-treated mice. $n = 4–5$. **f** BR.Ncf1* mice were treated i.p. with clodronate liposome to deplete macrophages, adoptively transferred with macrophages from BR.Ncf1* mice or BR.Ncf1*.Ym1$^{\Delta}$ mice, and injected i.p. with mannan to induce disease. $n = 6–7$. **g** Psoriasis lesion score and arthritis score were assessed. **h** BR.Ncf1* mice were tropically treated mannan on ears, and administrated i.d. with recombinant Ym1 protein or PBS control. $n = 10$. **i** Psoriasis lesion score was assessed. **j** Representative H&E images of ear skin sections taken on day 7 were shown and epidermal thickness was measured. $n = 8$. Data are presented as mean ± SEM. $^{*}p < 0.05$, $^{**}p < 0.01$.

response and drive the development of psoriatic lesions[24]. Therefore, we selected γδT cells to validate the role of Ym1.

To verify the regulation of γδT cells in Ym1 regulated skin inflammation, anti-γδT cells neutralizing antibody was used to deplete skin γδT cells intradermally in mice with IMQ treatment (Fig. 3d). The skin scaling was indeed decreased by the administration of neutralizing antibody (Fig. 3e). The infiltrating immune cells in the skin lesions were detected using flow cytometry, and the percentage of neutrophils and γδT cells were found to be reduced by the administration of neutralizing antibody (Fig. 3f). Particularly, the mRNA expression of *Il17* also showed marked decreased as neutralizing antibody treatment (Fig. 3g), whereas the epidermal thickness did not show significant difference (Fig. 3h). Taken together, it suggests that inhibition of IL-17 by blocking γδT cells partially suppress the immune response and disease.

Ym1 regulates keratin production in psoriatic skin

To better understand the role of Ym1 in the skin, we performed bulk RNA sequencing of skin tissues of BR.Ncf1* and BR.Ncf1*.Ym1$^{\Delta}$ mice treated with IMQ for seven days, which could provide a comprehensive overview of the transcriptional signature with influence on Ym1 (Fig. 4a). Through the comparison of two strains, 467 genes (including *Chil3*) were found to be upregulated in BR.Ncf1* mice compared to BR.Ncf1*.Ym1$^{\Delta}$ mice, while 134 genes were downregulated (Fig. 4b). When these mouse strains with differentially expressed genes (DEGs) were subjected to k-means clustering analysis, the Ym1 congenic mice had a different clustering compared to the BR.Ncf1* controls (Fig. 4c). Interestingly, eight chitinase and chitinase-like proteins were identified in skin, including *Chil1*, *Chil3* (Ym1), *Chil4* (Ym2), *Chil5, Ovgp1, Chid1, Ctbs* and *Chit1*, and Ym1 was the only one showing expression difference during disease which is resulted from *Chil3* polymorphism within these two strains (Fig. 4d).

Importantly, gene ontology and pathway analyses on all DEGs indicated the predominant involvement of intermediate filament or keratin filament (Fig. 4e). A total of 65 differentially-expressed genes coding keratins and keratin-associated proteins in skins were compared among mice by using a VlnPlot tool, and enriched by using gene set enrichment analysis (GSEA) (Fig. 4f, g). Notably, the absence of Ym1 suppressed keratin production in lesional skin, underscoring the regulatory role of Ym1 in keratinization. Although these findings were not directly derived from KCs, keratins could be produced by KCs in the epidermal layer of the skin and are known to be involved in the proliferation and differentiation of KCs during psoriasis pathogenesis[28]. These observations collectively suggest the potential involvement of Ym1 in keratin production and the functional regulation of KCs in psoriasis. However, further cellular experiments are warranted to validate this hypothesis.

In addition, the immune niche in skin was sketched by the analysis of Immune Cell Abundance Identifier (ImmuCellAI), that is based on DEGs and could be an important supplement to flow cytometry analysis (Fig. 4h). It is obvious that the granulocytes especially neutrophils were notably accumulated in skin of BR.Ncf1* mice, which is consistent with the results of skin flow cytometry analysis. Interestingly, M2 macrophages tended to accumulate in Ym1 congenic mice, but the data within the group is relatively dispersed (Fig. 4h). To further validate it, we determined the M2 macrophages in lesional skin of IMQ-treated mice by flow cytometry. It was shown that seven days after IMQ treatment, the macrophage proportion in skin was not changed consistent with previous observation, however, both the proportion of Arg1^{+}MRC1^{+} M2 macrophages and the expression intensity of Arg1in skin macrophages were significantly higher in Ym1 congenic mice than those in BR.Ncf1* control mice (Supplementary Fig. 4a–d). Besides, GSEA also clustered the PPARγ pathway, indicating an enhancement of the PPARγ pathway in the absence of Ym1 (Fig. 4i). These data are consistent with our previous findings that Ym1 deficiency enhances an alternative activation of M2 macrophages through the PPARγ-STAT6 pathway[6].

Ym1 stimulation directly regulates keratinocyte functionality

Given that the aforementioned results implied Ym1's potential to regulate KCs in the context of psoriasis, it became imperative to validate this effect through in vitro experiments. To this end, we isolated and cultured primary KCs from Ym1 congenic mice. These cells were subsequently stimulated either with rYm1 at varying doses or with M5 cocktails (comprising TNF-α, IL-17a, Oncostatin M, IL-1α, and IL-22) as a comparative control. Notably, previous research has indicated that skin inflammation induced by the synergistic action of these cytokines (referred to as the M5 cytokine cocktail) recapitulates some key features of psoriasis[29], which is why this combination has been widely utilized in cellular experiments to mimic the inflammatory environment associated with the disease. A comprehensive investigation into the effects of Ym1 stimulation on KCs was conducted, with a particular focus on its impact on inflammation (as evidenced by the regulation of *Tnf*, *Il17ra*, and *Ccl20*), proliferation (assessed through the expression levels of *Krt14*, *Krt16*, and *Krt17*), and differentiation (examined via the expression of *Krt1*, *Lor*, and *Flg*)[20,30–33]. In the context of inflammatory factor regulation, M5 significantly induced the expression of *Tnf*, *Il17ra* and *Ccl20*, while Ym1 stimulation also notably upregulated the expression of *Tnf* and *Il17ra* (Fig. 5a, b). This suggests that, in addition to its effects on immune cells, Ym1 can directly target KCs to modulate their inflammatory responses, which is an important supplement to the mechanism of Ym1 mediating skin inflammation. Regarding proliferation, Ym1 significantly enhanced the expression of *Krt14* and *Krt16* but did not affect *Krt17*, whereas M5's effect was confined to the regulation of *Krt16* (Fig. 5a, c). These findings imply that Ym1 is implicated in the hyperproliferation of KCs. Conversely, Ym1 did not exhibit a significant influence on cell differentiation, in contrast to M5, which primarily regulated *Krt1* expression (Fig. 5a, d). Meanwhile, the protein levels of proliferation-related molecules were also validated by Western blotting (Fig. 5e). To further directly observe the effect of Ym1 on the proliferation of KCs, we conducted CCK-8 and EdU assays on mouse primary KC stimulated with rYm1 or M5 cocktail. Both sets of results consistently demonstrated that Ym1 could promote the proliferation of KC (Fig. 5f, g). Collectively, our results demonstrate that Ym1 is capable of regulating the functions of KCs, with a particularly more pronounced impact on promoting KC proliferation compared to its effect on KC differentiation.

Discussion

The *Chil3*/Ym1 locus is one of the few positioned polymorphisms controlling complex inflammatory diseases in mice. It was identified in segregating crosses of mouse strains[6,34,35] and is highly polymorphic with different functional copies in the wild mouse population, strongly arguing for natural selection. We have now found that allelic variants, leading to high expression of Ym1, promotes skin IL-17 production and regulates keratinocyte functionality, thereby contributing to psoriasis-like skin inflammation in mice.

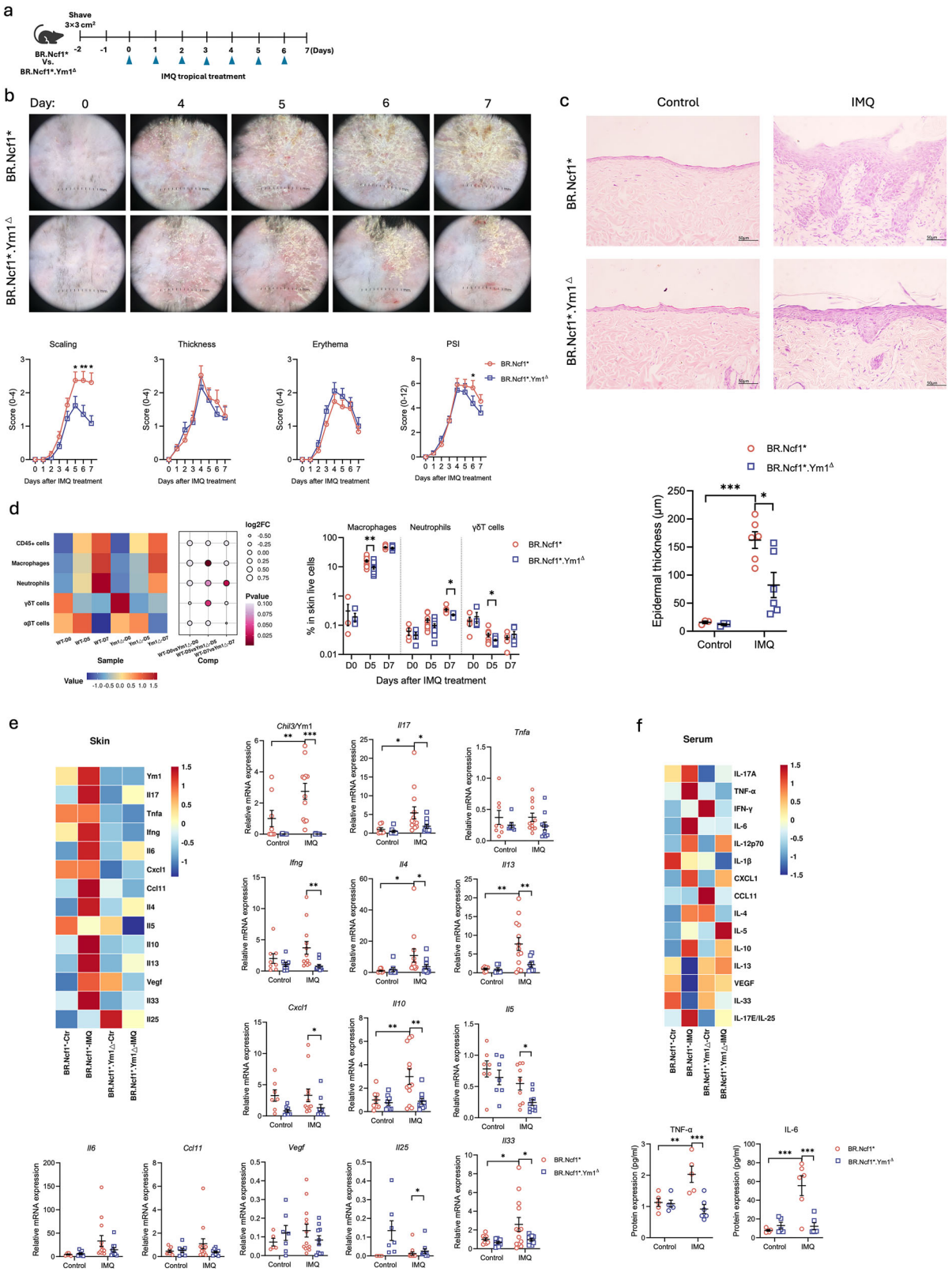

Fig. 2 | Macrophage Ym1 imbalances skin immune homeostasis in imiquimod (IMQ) -induced psoriasis-like dermatitis. a A scheme of imiquimod-induced psoriatic dermatitis using BR.Ncf1* mice and BR.Ncf1*.Ym1Δ mice **b** Images of skin manifestation on days 0, 4, 5, 6, and 7 in IMQ-treated mice. Disease severity was assessed from scaling, thickness and erythema daily, and the cumulative PSI score was calculated. $n = 18–19$. **c** Representative H&E images of skin sections taken on day 7 in IMQ-treated mice. Epidermal thickness was measured. $n = 3–6$. **d** Immune cells of skins taken on day 0, 5 and 7 in IMQ-treated mice were analyzed by flow cytometry. Heatmap of all cell populations and histogram of skin macrophages, neutrophils and γδT cells were shown. $n = 4–14$. **e** mRNA expression of cytokines in skin tissues taken on day 7 in IMQ-treated mice was determined by qPCR. Heatmap and histograms of all cytokines were shown. $n = 6–13$. **f** Cytokine concentration in serum taken on day 7 in IMQ-treated mice was determined by luminex. Heatmap of all cytokines and histograms of differentially expressed cytokines were shown. $n = 5–6$. Data are presented as mean ± SEM. $^*p < 0.05$, $^{**}p < 0.01$, $^{***}p < 0.001$.

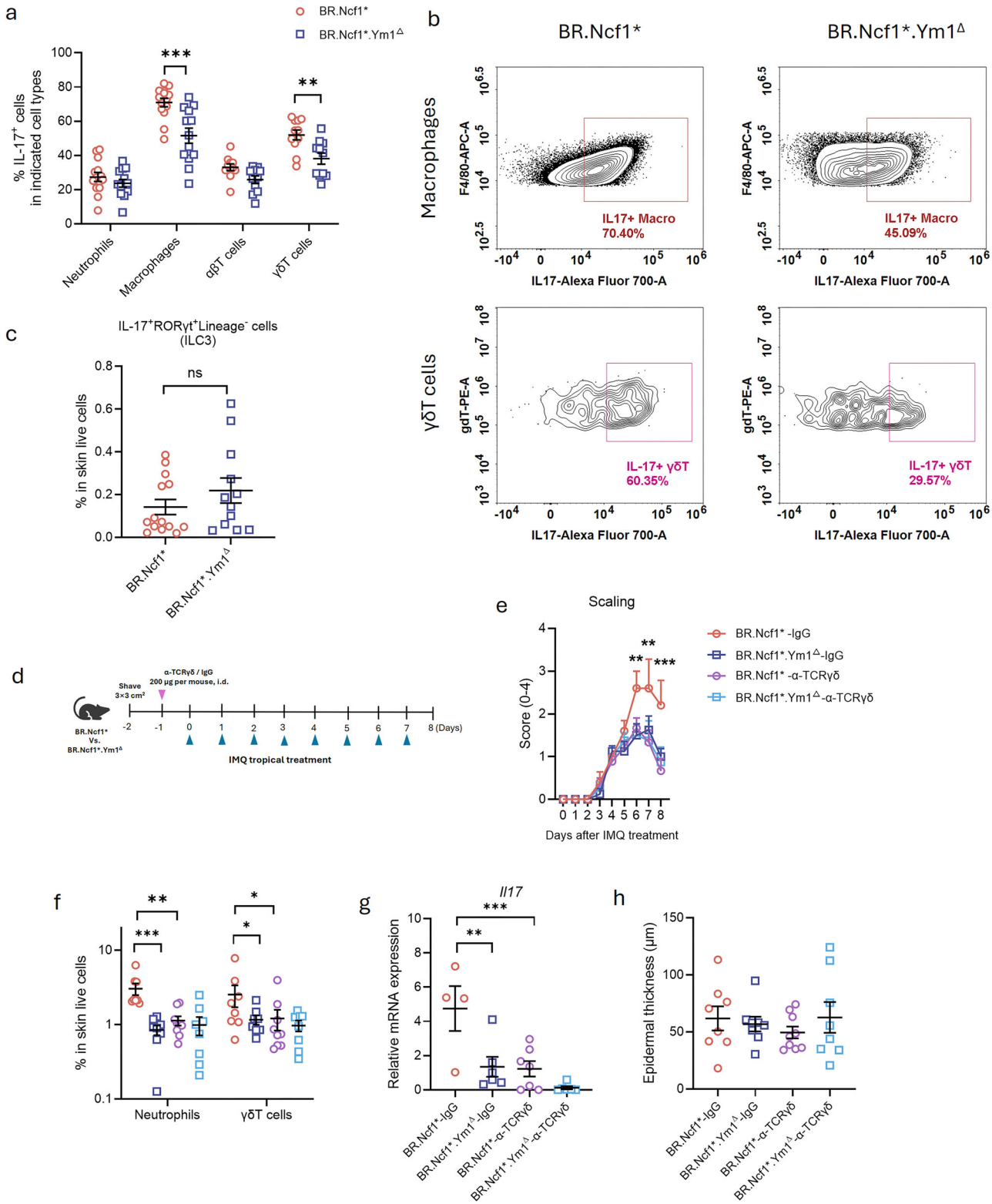

Fig. 3 | Ym1 regulating IL-17-producing cells contributes to skin inflammation. The proportion of IL-17 positive cells in immune cells of skin tissues taken on day 7 in IMQ-treated mice was determined by flow cytometry. The histogram (**a**) and representative plots (**b**) were shown. $n = 11–14$. **c** IL-17 positive ILC3 in skin tissue of IMQ-treated mice were also determined. **d** A scheme of imiquimod-induced psoriasis-like dermatitis model using BR.Ncf1* mice and BR.Ncf1*.Ym1Δ mice with treatment of anti-TCRγδ antibody. **e** Skin scaling score was assessed. $n = 5–9$. **f** Neutrophils and γδT cells in skin were analyzed by flow cytometry. $n = 8–9$. **g** The mRNA expression of *Il17* in skin tissue taken on day 8 in IMQ-treated mice was determined by qPCR. $n = 4–7$. **h** The lesional skin sections were stained by H&E, and the epidermal thickness was measured. $n = 8–9$. Data are presented as mean ± SEM. ns no significance, $^*p < 0.05$, $^{**}p < 0.01$, $^{***}p < 0.001$.

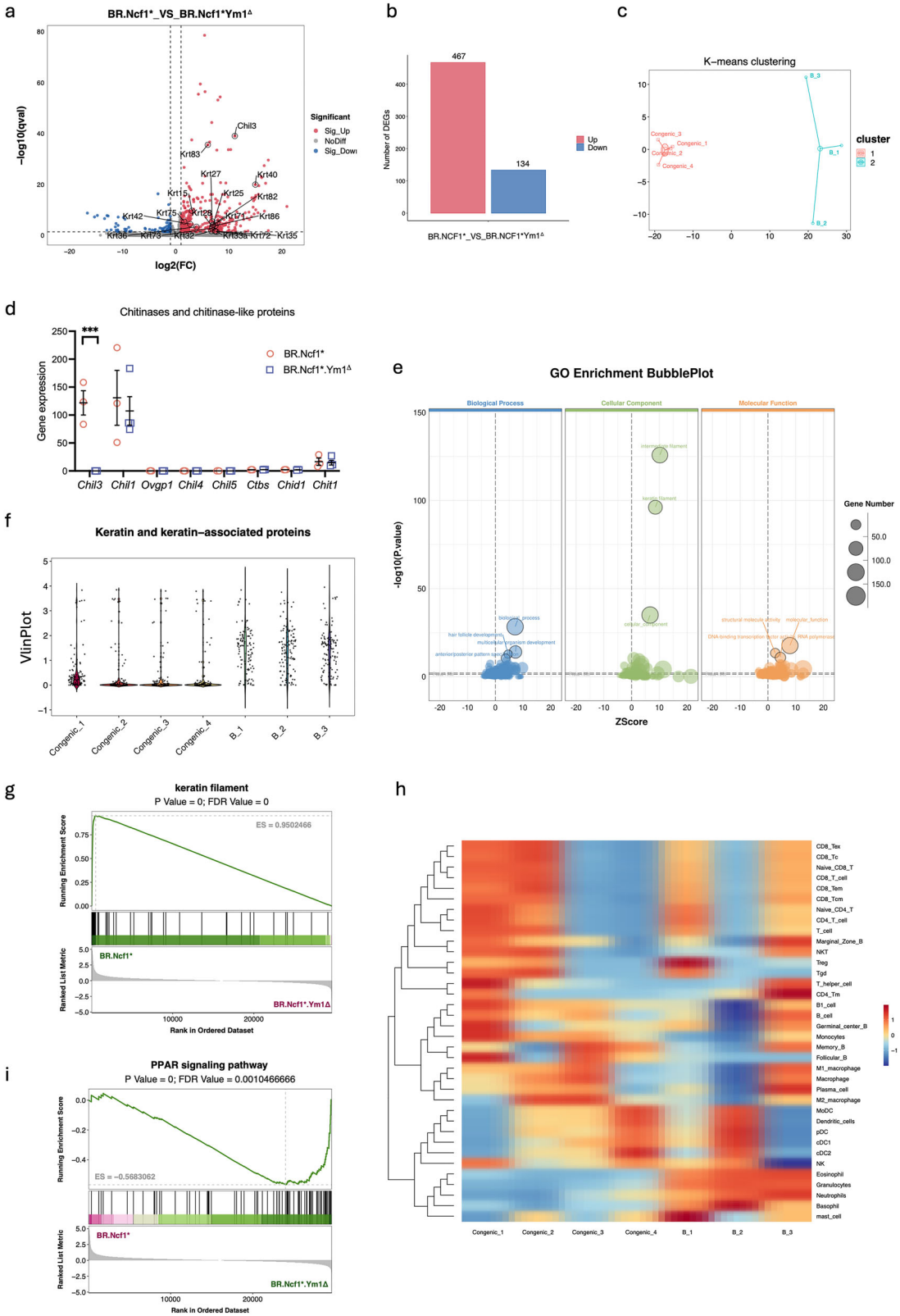

Fig. 4 | Ym1 regulates keratin production in lesional skin. RNA-seq analysis was performed using skin tissue of IMQ-treated BR.Ncf1* ($n = 3$, designated as B1, B2, and B3) and BR.Ncf1*.Ym1$^{\Delta}$ ($n = 4$, designated as Congenic1, Congenic2, Congenic3 and Congenic4) mice. The volcano plot of identified genes (**a**) and the number of differentially expressed genes (**b**) were shown. **c** K-means clustering of samples from two groups with different genotypes. **d** Gene expression of identified chitinases and chitinase-like proteins was compared between two groups. ***$p < 0.001$. **e** GO enrichment of differentially expressed genes. **f** Differentially expressed keratins and keratin-associated proteins were compared by a VlinPlot tool. **g** Keratin filament pathways were enriched by using gene set enrichment analysis (GSEA). **h** Immune cells in skin were sketched by the analysis of Immune Cell Abundance Identifier (ImmuCellAI). **i** PPAR pathways were enriched by GSEA. Data were analyzed by using the online OmicStudio tools (LC Bio Technology CO.,Ltd).

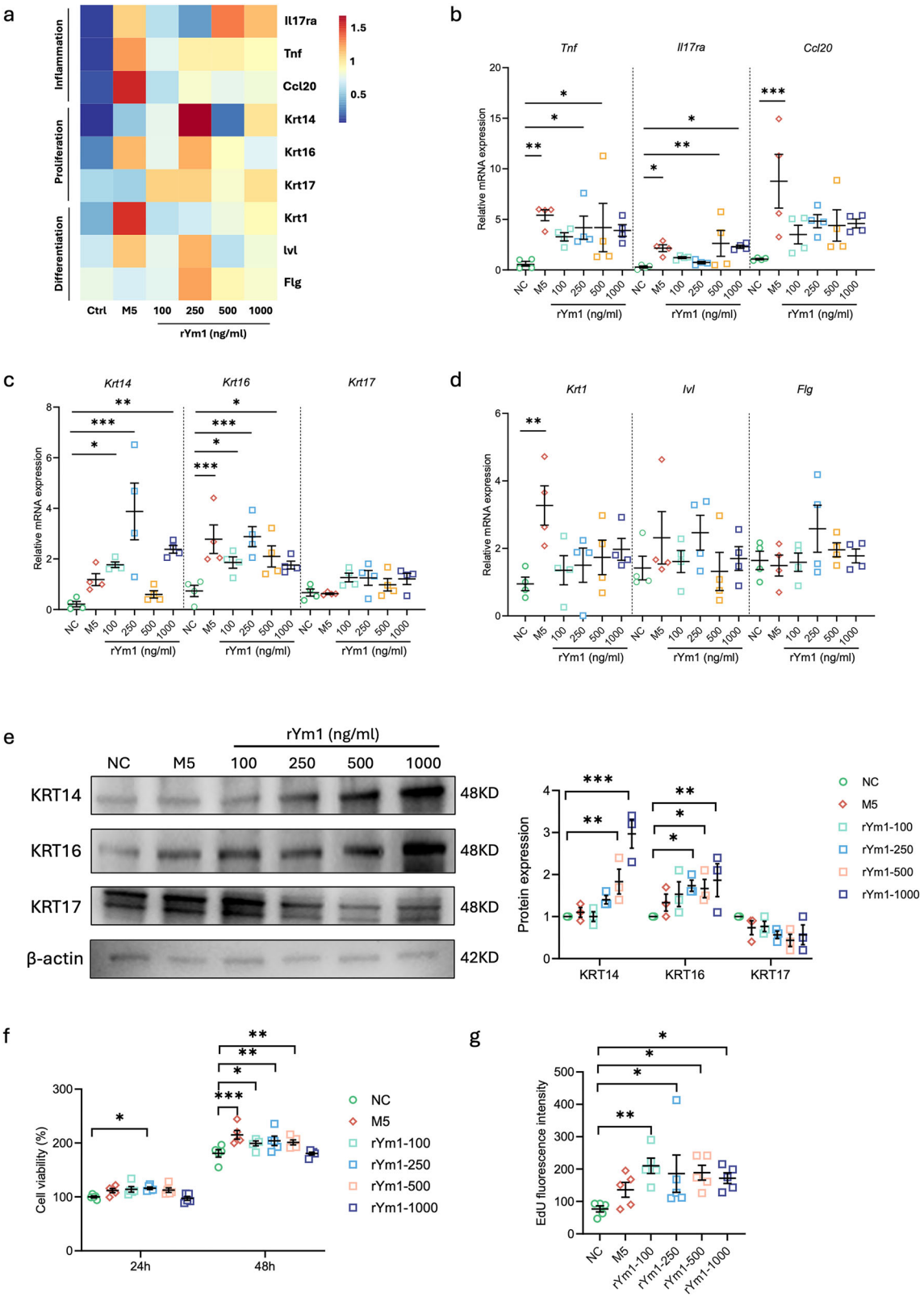

Fig. 5 | Ym1 regulates keratinocyte functionality. Primary keratinocytes from BR.Ncf1*.Ym1$^{\Delta}$ mice were stimulated by rYm1 proteins with different concentrations, or by M5 cytokine cocktails. The mRNA expression of genes related to inflammatory response, proliferation and differentiation were determined by qPCR after 24 h stimulation, shown in heatmap (**a**) and histograms (**b**–**d**). $n = 4$. **e** Proliferation-related Keratins in cells was also determined by Western blotting. $n = 3$. **f** Cell viability was measured by CCK-8 assay in KCs with 24 h and 48 h stimulation. $n = 5$. **g** Cell proliferation was determined by EdU assay in KCs with 48 h stimulation. $n = 5$. Data are presented as mean ± SEM. $^{*}p < 0.05$, $^{**}p < 0.01$, $^{***}p < 0.001$.

Psoriasis is a chronic inflammatory disease in skin, and various animal models (spontaneous, genetically engineered, human skin transplant, and induced mouse models) are being used for studies of pathogenic mechanisms and potential drug testing[36]. Among them, IMQ-induced model is the most commonly used, which simulates psoriasis-like inflammation in local area of skin, allowing us to better evaluate skin inflammation in those region[37]. The disparity between this and the generalized occurrence of the disease affecting the entire skin in humans may also indicate differences in the underlying mechanisms. Alternatively, the MIP model, which systematically involves the entire skin, effectively addresses this issue. Although it remains uncertain whether this polysaccharide, a common cell wall component of *Saccharomyces cerevisiae*, is a risk factor for human diseases, it excellently mimics human diseases in clinical, pathological, and biochemical aspects[7]. It is noteworthy that the two models possess distinct immune regulatory mechanisms, with different expression patterns of IL-17 family molecules, suggesting that combining their use may lead to better outcomes[38]. Thus, we tested the role of Ym1 using the Ym1-deficient congenic mice, and both models confirmed the pathogenic effect of Ym1.

Both innate and adaptive immune systems are involved in the pathogenesis of psoriasis, and myeloid cells, T cells, and KCs have key functions in the process[39,40]. Eighty percent of genes significantly elevated in psoriasis lesions can be explained by KC activity and infiltration by T-cells and macrophages[41]. These crucial cell types are possible downstream targets of the Ym1 regulated pathogenic effect. As a secretory protein, Ym1 is predominantly expressed by macrophages, though its expression has also been reported in neutrophils[42]. Importantly, Ym1, along with Arg1 and Fizz1, has been identified as a marker of M2 macrophages in mice, although the exact physiological function of Ym1 remains elusive[43]. In this study, the co-localization of macrophages and Ym1 in skin lesions, along with the observed differences in skin macrophages during the early stages of the disease as Ym1 deficiency, suggests a regulatory role of Ym1 on macrophages. Specifically, our study corroborates prior insights into Ym1-mediated macrophage regulation, particularly its role in modulating alternative macrophage activation via the STAT6-PPARγ pathway[6]. Notably, the PPARγ pathway was also enriched in our RNA sequence analysis in skin. Furthermore, the macrophage adoptive transfer experiment underscores once again the pivotal role of Ym1-regulated macrophages in the disease process.

Due to the involvement of M2 macrophages and type 2 immunity, Ym1 has been linked to many disease models in mice. Although the exact mechanisms remain unclear, its immune regulatory role cannot be overlooked. It has been reported that Ym1 promoted IL-17–mediated neutrophilia involving in nematode killing and host damage in mice[10], and also Ym1 in neutrophils contributed to a cardioprotective effect protection by promoting M2 polarization[44]. Here we also analyzed the immune regulation in the skin or draining lymph node in disease through flow cytometry and RNA sequencing, and found that neutrophils, as potential Ym1 effector cells, might be involved in the progression of the disease. Of particular interest, we also found that Ym1 regulated the production of IL-17 in various IL-17-producing cells like γδT cells. Since both the IMQ model and the MIP model were found to be γδT cell-dependent[7,45], we partially depleted this population in vivo through antibody administration and observed a significant inhibition in IL-17 production and disease severity. It is well-accepted that IL-23/IL-17 axis play crucial roles in the pathogenesis of psoriasis and biologic therapies targeting it have transformed the disease treatment, therefore, it is evident that the regulation of IL-17 producing cells is one of the crucial mechanisms by which Ym1 mediates the pathogenesis of psoriasis-like skin inflammation in mice.

KCs play a central role in the pathogenesis of psoriasis through their hyperproliferation, differentiation defects, inflammatory cytokine production, and interactions with immune cells[1]. In our RNA sequencing data, the enrichment of keratinization pathways suggests a potential role for Ym1 in targeting KCs, implying its involvement in other mechanisms. We therefore evaluated the effects of Ym1 using primary KCs from three perspectives, inflammation, proliferation and differentiation, and confirmed its primary impacts on the inflammatory response and hyperproliferation of KCs. This finding serves as a crucial complement to the mechanism by which Ym1 influences KCs through immune cells, shedding further light on its regulatory role in skin physiology. In addition, we found it intriguing that Ym1 regulated the expression of proliferation-related keratins, Krt14 and Krt16, but did not affect Krt17. This discrepancy may arise from distinct regulatory pathways or competition for shared transcription factors. However, future investigations are warranted to fully elucidate the precise mechanisms by which Ym1 influences KC function, including potential Ym1-binding receptors and the signaling pathways they mediate.

In conclusion, we have validated that Ym1 is instrumental in driving the development of psoriasis-like skin inflammation in mice, operating in a macrophage-dependent manner, orchestrating IL-17-producing cells and keratinocyte functionality. Although Ym1 is a protein specific to rodents, the chitinases and CLPs as a group display a high degree of sequence conservation, indicating that they may possess shared biological functions. Furthermore, reports have indicated that YKL-40 and CHIT1, which are paralogs of Ym1, are involved in psoriasis, although the underlying mechanisms remain unclear[46,47]. Our investigation of Ym1, while specific to murine models, will help us to understand the functional roles and mechanistic underpinnings of human chitinases and CLPs in psoriasis pathogenesis. By leveraging insights from this murine-specific protein, we aim to decode conserved pathways relevant to human chitinase biology, thereby establishing a translational foundation for developing novel diagnostic biomarkers and targeted therapies for psoriasis in future.

Methods

Mouse strains

B10.RIII H2r MHC (major histocompatibility complex) haplotype-bearing mice were originated in J. Klein's laboratory (Max Planck Institute for Biology, Tübingen). BR.Ym1$^{\Delta}$ mice were a congenic strain in B10.RIII background carrying a 2-Mb RIIIS/J fragment, leading to Ym1 deficiency due to *Chil3* polymorphism[6]. Notably, *Chil3* haplotypes are classified as the B haplotype in C57BL strains, such as B10.RIII, whereas they are designated as the RIII haplotype in the RIIIS/J strain and our congenic mouse line. Mice were then intercrossed with an *Ncf1*^{m1j} mutant strain (Ncf1* for short) to generate the BR.Ncf1*.Ym1$^{\Delta}$ strain, since it could increase the psoriasis susceptibility and also cause the manifestation of symptoms of psoriatic arthritis in MIP[22]. BR.Ym1$^{\Delta}$ and BR.Ncf1*.Ym1$^{\Delta}$ strains were established in Karolinska Institutet, and maintained in the Experimental Animal Center in Xi'an Jiaotong University, in a temperature-controlled environment at 22 °C under 12 h light/dark cycles.

For all experiments, 10- to 14-week-old age-matched male congenic and wild-type littermate controls have been used. All animal experiments were performed according to the guidelines of the Institutional Animal Use and approved by the Institutional Animal Ethics Committee of Xi'an Jiaotong University (No.2021-1071). We have complied with all relevant ethical regulations for animal use.

Mannan-induced psoriasis-like dermatitis

Mice were injected intraperitoneally with 20 mg of mannan (Sigma) to induce psoriasis-like dermatitis and arthritis, and were scored daily for the psoriasis lesion[7]. In another experiment, mice were topically treated with mannan on ears (5 mg in 50 µl incomplete Freund's adjuvant (IFA) per ear) for three consecutive days to induce psoriatic dermatitis[48], and intradermally administrated with 5 µg rYm1 protein or PBS. The severity of the psoriasis-like skin manifestations for MIP models was monitored on a 15-score system, in which ears or each paw was evaluated by a scale ranging from 1 to 3 (1, weak skin peeling; 2, moderate skin peeling; and 3, heavy skin peeling with some hair loss). Arthritis development and severity were monitored by recording the macroscopic clinical score as previous described[6].

Macrophage adoptive transfer

Bone marrow cells were washed out from BR.Ncf1* mice and BR.Ncf1*.Ym1$^{\Delta}$ mice respectively, and were treated with M-CSF (10 ng/ml,

SinoBiological) for seven days to differentiate to macrophages for adoptive transfer. BR.Ncf1* mice, serving as recipients, were injected intraperitoneally with either 500 μl of clodronate liposomes (Liposoma) and control liposomes for macrophage depletion. After seven days, these mice were subsequently subjected to adoptive transfer of macrophages (3×10^6 cells per mouse) and induction of MIP model (intraperitoneally injected model).

IMQ-induced psoriasis-like dermatitis

Mice were treated with a daily dose of 62.5 mg imiquimod (IMQ) cream (Sichuan Med-Shine Pharmaceutical Co., Ltd.) on the shaved back of 3.0 cm × 3.0 cm for 7 consecutive days to induce psoriasis-like dermatitis. The control mice were treated similarly with Vaseline cream. For disease evaluation, a blinded observer measured the thickness of the dorsal skins by a vernier caliper daily, and photographed the back skin with a dermoscope. Psoriasis Severity Index (PSI) scores were used to evaluate the severity of skin lesions every day, which were graded from 0 to 4 for erythema, thickness and scaling[49].

Depletion of γδT cell in vivo

Antibody against γδT cells or isotype IgG (200 μg per mouse, BioXCell) was injected intradermally to BR.Ncf1* mice and BR.Ncf1*.Ym1$^{\Delta}$ mice. One day later, mice were subjected to the induction of IMQ-induced psoriatic dermatitis model.

Immunohistochemistry

Skin tissues were fixed in 4% paraformaldehyde, embedded in paraffin, and stained with hematoxylin-eosin (H&E) reagent. The thickness of epidermal and the area of Munro's microabscesses were assessed by SlideViewer (3DHISTECH Ltd.).

For immunofluorescence staining, skin sections were stained with rabbit anti-Ym1 antibody (Abcam, ab93034), rat anti-mouse F4/80 antibody (Thermo Fisher, 14-4801-82), followed by rhodamine or FITC -conjugated secondary antibody (Jackson ImmunoResearch) for co-localization. DAPI (Bioworld Technology, China) was used to stain the nuclei. The images were captured by multiphoton microscope (SP8 DIVE, Leica). Leica Las X3.5.7 software was employed for both acquisition and analysis of immunofluorescence staining.

Flow cytometry

Skin tissues were cut into small pieces and digested with collagenase type I (2.6 mg/ml, Sigma) and DNase I (0.1 mg/ml, Sigma). The digested skin tissues, or draining lymph nodes were grinded and filtered by a 40 μm cell strainer to prepare single cell suspension. Then, cells were stained with LIVE/DEAD fixable violet stain kit (Thermo Fisher), and labeled with anti-mouse- BV785-CD45.2 (Cat No. 109839, BioLegend), anti- mouse-AF700-TCRβ (Cat No. 109224, BioLegend), anti-mouse-FITC-CD3 (Cat No. 561798, Becton Dickinson), anti-mouse-PE-Cy5-CD4 (Cat No. 100514, BioLegend), anti-mouse-BV711-CD8 (Cat No. 100759, BioLegend), anti-mouse-APC-CD11b (Cat No. 101212, BioLegend), anti-mouse-FITC-F4/80 (Cat No. 123108, BioLegend), anti-mouse-Pacific blue-Ly6G (Cat No. 127612, BioLegend), anti-mouse-PE-γδT (Cat No. 553178, Becton Dickinson), anti-mouse-FITC-Arg1 (Cat No. IC5868F, R&D), and anti-mouse-PE-MRC1 (Cat No. 141706, BioLegend). For intracellular staining, cells were fixed and permeated by using BD Cytofix/Cytoperm before intracellular antibody incubation. For cytokine staining, cells were pre-treated with phorbol 12-myristate 13-acetate (PMA, 100 ng/ml, Sigma), ionomycin (1 mg/ml, Sigma) and brefeldin A (10 mg/ml, Selleck) for 4 h, fixed and permeated by using BD Cytofix/Cytoperm after membrane staining, and labeled with anti-mouse-AF700-IL-17A (Cat No. 560820, Becton Dickinson). For ILC3 analysis, skin cells were stained with anti-mouse-BV785-CD45.2 (Cat No. 109839, BioLegend), PerCP-Cy™5.5 mouse lineage antibody cocktail (Cat No. 561317, Becton Dickinson), after fixation and permeation, were subsequently stained with anti-mouse-BV650-RORt (Cat No. 564722, Becton Dickinson) and anti-mouse-AF700-IL-17A (Cat No. 560820, Becton Dickinson). Finally, samples were detected and analyzed with an Agilent NovoCyte 3005 flow cytometer. Gating strategy of cells in flow cytometry is shown in Supplementary Fig. 5. The cell population referred to is displayed in proportion to live cells or in absolute cell counts. For cell counts, the total number is counted before staining and converted after proportion analysis by flow cytometry.

RNA quantitation by qPCR and bulk RNA sequencing

Total RNA from the skin tissues and primary cells was isolated by using TRI Reagent (Sigma), and cDNA was synthesized using RevertAid First Strand cDNA Synthesis Kit (Thermo Fisher). Real-time qPCR was performed by QuantStudio 5 (Applied Biosystems) with FastStart Universal SYBR Green Master (Roche). The relative gene expression normalized by β-*actin* was calculated with the $2^{-\Delta\Delta CT}$ method. The primers used were described in Supplementary Table 1.

For bulk RNA sequencing, skin tissues of BR.Ncf1* mice and BR.Ncf1*.Ym1$^{\Delta}$ mice with IMQ-induced psoriasis on day 7 were collected. The RNA libraries were sequenced on the illumina Novaseq™ 6000 platform by LC Bio Technology CO.,Ltd (Hangzhou), and data were analyzed by using the online OmicStudio tools.

Luminex

For Luminex assay, selected cytokines were quantified in serum samples of mice using a 15-plex Luminex panel (LXSAMSM-15, R&D Systems). The sample was diluted twice and the plate was detected by Luminex X-200. This assay was assisted by Univ-Bio Company (Shanghai).

Primary keratinocytes

To isolate primary murine KCs, the skin from the tails of adult BR.Ncf1*.Ym1$^{\Delta}$ mice was cut into small pieces and then suspended on Dispase II (Sigma-Aldrich cat. D4693, 4 mg/ml) 7 h at 4 °C. Then the epidermis was peeled and placed into 0.25% trypsin for 10 min at 37 °C. The digestion was terminated by using EpiLife Medium (GIBCO cat. MEPI500CA) containing 1% fetal bovine serum (ExCell Bio cat. FSP500), and the epidermal cells were seeded in culture plates pre-coated with collagen (Solarbio, C8062, 0.012 mg/ml) and cultured in EpiLife Medium supplemented with human keratinocyte growth supplement (GIBCO cat. S0015), 100 U/ml of penicillin, and 100 μg/ml of streptomycin. Non-adherent cells and dead cells are removed through washing. Besides, the purity of the isolated cells was assessed via flow cytometry using staining with antibodies against KRT14 (anti-mouse-CoraLite488-KRT14, Cat No. CL488-60320, Proteintech) and CD45 (anti-mouse-BV785-CD45.2, Cat No. 109839, BioLegend). KCs that were KRT14^{+}CD45^{-}, with a purity exceeding 95%, were utilized in the subsequent cell experiments (Supplementary Fig. 6). Then, the primary KCs were treated with 100, 250, 500 and 1000 ng/ml of rYm1 protein, or with 10 ng/ml of M5 cocktail (IL-17A, IL-22, Oncostatin M, IL-1α, and TNF-α) for 24 h[29].

Western blotting

RIPA lysis buffer (Beyotime, China) was used to extract proteins from mouse primary keratinocytes. The protein concentrations were determined with a Pierce BCA Protein Assay Kit (Thermo Fisher Scientific, USA). Two micrograms of total protein were loaded into each well of a 12% gel and subjected to SDS-PAGE. Protein was transferred to 0.45 μm nitrocellulose membranes. The membranes were blocked with 10% nonfat milk in Tris-buffered saline-Tween-20 and then incubated with rabbit polyclonal antibodies against Krt14, Krt16 and Krt17 (Proteintech) at 4 °C overnight. β-actin (Proteintech) was used as the loading control. The membranes were then incubated with Goat Anti-Rabbit IgG H&L-HRP (Zenbio, China) for 1 h at room temperature, and developed via enhanced chemiluminescence (ECL) plus Western blotting detection system.

Cell proliferation

rYm1 was used to stimulate primary KCs in vitro, and cell viability was measured by CCK-8 assay while cell proliferation was determined by 5-Ethynyl-2′-deoxyuridine (EdU) assay. For CCK-8 assay, we seeded KCs

onto 96-well plates at a density of 2000 cells per well. Then, the medium was replaced with fresh medium containing 10 ng/ml M5 or various concentrations (0, 100 ng/ml, 250 ng/ml, 500 ng/ml, and 1000 ng/ml) of rYm1. After 24 h and 48 h incubation, 10 μl of CCK8 solution (NCM Biotech, China) was added to each well. Following 1 h incubation at 37 °C, the absorbance of each well at 450 nm was determined.

EdU assay was undertaken with BeyoClick™ EdU Cell Proliferation Kit with Alexa Fluor 594 (Beyotime, Shanghai, China). Primary KCs were treated with above-mentioned stimulators for 48 h, and then EdU solution was used to incubate cells for 2 h. After washing, Click Reaction Solution was used to incubate cells for 30 min. Finally, the fluorescence intensity of each well (λ_{Ex} = 590 nm, λ_{Em} = 615 nm) was determined by using a microplate reader (PerkinElmer, EnSpire 2300).

Statistics and reproducibility

Quantitative data are expressed as means ± SEM. The statistical analysis of differences was performed using Student's *t* test between two experimental groups or one-way analysis of variance (ANOVA) for more than two groups. A *P* value of less than 0.05 was considered significant. Animal numbers are indicated in the figures. Experiments are reproduced 2–3 times. All data shown in figures are biological replications rather than technical replications.

Reporting summary

Further information on research design is available in the Nature Portfolio Reporting Summary linked to this article.

Data availability

RNA sequence data have been deposited in Genome Sequence Archive (GSA) with accession number CRA028275[50,51]. The uncropped and unedited blot images have been provided in Supplementary Fig. 7. The numerical source data for graphs and charts are shown in Supplementary Data 1. All other data that support the findings of this study are available from the corresponding author upon reasonable request.

Received: 26 January 2025; Accepted: 29 July 2025;
Published online: 08 August 2025

References

1. Sieminska, I., Pieniawska, M. & Grzywa, T. M. The immunology of psoriasis-current concepts in pathogenesis. *Clin. Rev. Allergy Immunol.* **66**, 164–191 (2024).
2. Armstrong, A. W. & Read, C. Pathophysiology, clinical presentation, and treatment of psoriasis: a review. *JAMA* **323**, 1945–1960 (2020).
3. Chen, L. & Tsai, T. F. HLA-Cw6 and psoriasis. *Br. J. Dermatol* **178**, 854–862 (2018).
4. Elder, J. T. PSORS1: linking genetics and immunology. *J. Investig. Dermatol.* **126**, 1205–6 (2006).
5. Capon, F. The genetic basis of psoriasis. *Int. J. Mol. Sci.* **18**, 2526 (2018).
6. Zhu, W. et al. Natural polymorphism of Ym1 regulates pneumonitis through alternative activation of macrophages. *Sci. Adv*. **6**, eaba9337 (2020).
7. Khmaladze, I. et al. Mannan induces ROS-regulated, IL-17A-dependent psoriasis arthritis-like disease in mice. *Proc. Natl. Acad. Sci. USA* **111**, E3669–78 (2014).
8. Zhong, J. et al. Mannan-induced Nos2 in macrophages enhances IL-17-driven psoriatic arthritis by innate lymphocytes. *Sci. Adv.* **4**, eaas9864 (2018).
9. Lee, C. G. et al. Role of chitin and chitinase/chitinase-like proteins in inflammation, tissue remodeling, and injury. *Annu. Rev. Physiol.* **73**, 479–501 (2011).
10. Sutherland, T. E. et al. Chitinase-like proteins promote IL-17-mediated neutrophilia in a tradeoff between nematode killing and host damage. *Nat. Immunol.* **15**, 1116–25 (2014).
11. Osborne, L. C. et al. Coinfection. Virus-helminth coinfection reveals a microbiota-independent mechanism of immunomodulation. *Science* **345**, 578–82 (2014).
12. Sutherland, T. E. et al. Ym1 induces RELMalpha and rescues IL-4Ralpha deficiency in lung repair during nematode infection. *PLoS Pathog.* **14**, e1007423 (2018).
13. Ikeda, N. et al. Emergence of immunoregulatory Ym1(+)Ly6C(hi) monocytes during recovery phase of tissue injury. *Sci Immunol.* **3**, eaat0207 (2018).
14. Cai, Y. et al. Ym1/2 promotes Th2 cytokine expression by inhibiting 12/15(S)-lipoxygenase: identification of a novel pathway for regulating allergic inflammation. *J. Immunol.* **182**, 5393–9 (2009).
15. Gu, J. et al. Therapeutic response to HMGB1-R3V6-conjugated Ym1/Ym2 siRNA complex in ovalbumin-induced murine asthma. *J. Control Release* **213**, e102 (2015).
16. Starossom, S. C. et al. Chi3l3 induces oligodendrogenesis in an experimental model of autoimmune neuroinflammation. *Nat. Commun.* **10**, 217 (2019).
17. Yamamoto, S. et al. Atherosclerosis following renal injury is ameliorated by pioglitazone and losartan via macrophage phenotype. *Atherosclerosis* **242**, 56–64 (2015).
18. Hayes, E. M. et al. Classical and alternative activation and metalloproteinase expression occurs in foam cell macrophages in male and female apoe null mice in the absence of T and B lymphocytes. *Front. Immunol.* **5**, 537 (2014).
19. Shaul, M. E. et al. Dynamic, M2-like remodeling phenotypes of CD11c + adipose tissue macrophages during high-fat diet-induced obesity in mice. *Diabetes* **59**, 1171–81 (2010).
20. Tollenaere, M. A. X. et al. Signalling of multiple interleukin (IL)-17 family cytokines via IL-17 receptor A drives psoriasis-related inflammatory pathways. *Br. J. Dermatol.* **185**, 585–594 (2021).
21. Fragoulis, G. E., Siebert, S. & McInnes, I. B. Therapeutic targeting of IL-17 and IL-23 cytokines in immune-mediated diseases. *Annu. Rev. Med.* **67**, 337–53 (2016).
22. Zhong, J., Li, Q. & Holmdahl, R. Natural loss-of-function mutations in Qa2 and NCF1 cause the spread of mannan-induced psoriasis. *J. Investig. Dermatol.* **141**, 1765–1771.e4 (2021).
23. Jiang, W. et al. Keratinocyte-to-macrophage communication exacerbate psoriasiform dermatitis via LRG1-enriched extracellular vesicles. *Theranostics* **14**, 1049–1064 (2024).
24. Liu, N. et al. Dynamic trafficking patterns of IL-17-producing gammadelta T cells are linked to the recurrence of skin inflammation in psoriasis-like dermatitis. *EBioMed.* **82**, 104136 (2022).
25. Dyring-Andersen, B. et al. Interleukin (IL)-17A and IL-22-producing neutrophils in psoriatic skin. *Br. J. Dermatol.* **177**, e321–e322 (2017).
26. Hou, Y. et al. IL-23-induced macrophage polarization and its pathological roles in mice with imiquimod-induced psoriasis. *Protein Cell* **9**, 1027–1038 (2018).
27. Bielecki, P. et al. Skin-resident innate lymphoid cells converge on a pathogenic effector state. *Nature* **592**, 128–132 (2021).
28. Jiang, Y. et al. Cytokinocytes: the diverse contribution of keratinocytes to immune responses in skin. *JCI Insight* **5**, e142067 (2020).
29. Guilloteau, K. et al. Skin inflammation induced by the synergistic action of IL-17A, IL-22, oncostatin M, IL-1alpha, and TNF-alpha recapitulates some features of psoriasis. *J. Immunol.* **184**, 5263–5270 (2010).
30. Moll, R., Divo, M. & Langbein, L. The human keratins: biology and pathology. *Histochem. Cell Biol.* **129**, 705–33 (2008).
31. Sandilands, A. et al. Filaggrin in the frontline: role in skin barrier function and disease. *J. Cell Sci.* **122**, 1285–94 (2009).
32. Homey, B. et al. Up-regulation of macrophage inflammatory protein-3 alpha/CCL20 and CC chemokine receptor 6 in psoriasis. *J. Immunol.* **164**, 6621–32 (2000).
33. Schmidt, A. D. et al. Involucrin modulates vitamin D receptor activity in the epidermis. *J. Investig. Dermatol.* **143**, 1052–1061.e3 (2023).

34. Johannesson, M. et al. Identification of epistasis through a partial advanced intercross reveals three arthritis loci within the Cia5 QTL in mice. *Genes Immun.* **6**, 175–85 (2005).
35. Johannesson, M. et al. Gene expression profiling of arthritis using a QTL chip reveals a complex gene regulation of the Cia5 region in mice. *Genes Immun.* **6**, 575–83 (2005).
36. Schon, M. P., Manzke, V. & Erpenbeck, L. Animal models of psoriasis-highlights and drawbacks. *J. Allergy Clin. Immunol.* **147**, 439–455 (2021).
37. Swindell, W. R. et al. Imiquimod has strain-dependent effects in mice and does not uniquely model human psoriasis. *Genome Med.* **9**, 24 (2017).
38. Wu, H. et al. Comparative studies on mannan and imiquimod induced experimental plaque psoriasis inflammation in inbred mice. *Clin. Exp. Immunol.* **211**, 288–300 (2023).
39. Griffiths, C. E. M. et al. Psoriasis. *Lancet* **397**, 1301–1315 (2021).
40. Liu, S. et al. Triggers for the onset and recurrence of psoriasis: a review and update. *Cell Commun. Signal.* **22**, 108 (2024).
41. Swindell, W. R. et al. Dissecting the psoriasis transcriptome: inflammatory- and cytokine-driven gene expression in lesions from 163 patients. *BMC Genom.* **14**, 527 (2013).
42. Kang, Q. et al. An update on Ym1 and its immunoregulatory role in diseases. *Front. Immunol.* **13**, 891220 (2022).
43. Misson, P. et al. Markers of macrophage differentiation in experimental silicosis. *J. Leukoc. Biol.* **76**, 926–32 (2004).
44. Dong, Y. et al. Single-cell profile reveals the landscape of cardiac immunity and identifies a cardio-protective Ym-1(hi) neutrophil in myocardial ischemia-reperfusion injury. *Sci. Bull.* **69**, 949–967 (2024).
45. Zarin, P. et al. Treg cells require Izumo1R to regulate gammadeltaT cell-driven inflammation in the skin. *Proc. Natl. Acad. Sci. USA* **120**, e2221255120 (2023).
46. Khashaba, S. A. et al. Serum YKL-40 and IL 17 in psoriasis: reliability as prognostic markers for disease severity and responsiveness to treatment. *Dermatol. Ther.* **34**, e14606 (2021).
47. Ilanbey, B. et al. A novel marker of systemic inflammation in psoriasis and related comorbidities: chitotriosidase. *Turk. J. Med. Sci.* **51**, 2318–2323 (2021).
48. Li, Y. et al. Human NCF1(90H) Variant Promotes IL-23/IL-17-Dependent Mannan-Induced Psoriasis and Psoriatic Arthritis. *Antioxidants* **12**, 1348 (2023).
49. Li, F. et al. Topical Treatment of Colquhounia Root Relieves Skin Inflammation and Itch in Imiquimod-Induced Psoriasiform Dermatitis in Mice. *Mediators Inflamm.* **2022**, 5782922 (2022).
50. Chen, T. et al. The Genome Sequence Archive Family: Toward Explosive Data Growth and Diverse Data Types. *Genomics Proteomics Bioinformatics* **19**, 578–583 (2021).
51. CNCB-NGDC Members and Partners. Database Resources of the National Genomics Data Center, China National Center for Bioinformation in 2025. *Nucleic Acids Rres*. **53**, D30–D44 (2025).

Acknowledgements

We are very grateful for the financial support from the National Natural Science Foundation of China (82171724, 82370460, 82171784, W2431021 and 82471830), the Natural Science Foundation of Shaanxi Province (2025JC-JCQN-096 and 2022JQ-752), the Key Research and Development Program of Shaanxi (2024GH-ZDXM-34) as well as Vetenskapsrådet (2024-02575) and Leo foundation (LF-OC-22-001023).

Author contributions

WZhang: designing research studies, performing experiments, acquiring of data, data analysis, writing the manuscript. F.L.: designing research studies, performing experiments, acquiring data, data analysis, revising the manuscript. Y.W.: performing experiments, acquiring of data, data analysis. M.F.: performing experiments, acquiring of data, data analysis. YZhao: performing experiments, acquiring of data, data analysis. Y.G.: performing experiments, acquiring of data, data analysis. YZhou: designing research studies, data analysis, writing and revising the manuscript. S.L.: designing research studies, data analysis, revising the manuscript. RH: designing research studies, data analysis, revising the manuscript. M.L.: designing research studies, data analysis, writing and revising the manuscript. WZhu: supervision and overall responsibility, designing research studies, writing and revising the manuscript. All authors ensure the accuracy of this work.

Competing interests

The authors declare no competing interests.

Ethical approval

All animal experiments were performed according to the guidelines of the Institutional Animal Use and approved by the Institutional Animal Ethics Committee of Xi'an Jiaotong University (No.2021-1071).

Additional information

Supplementary information The online version contains supplementary material available at https://doi.org/10.1038/s42003-025-08628-1.

Correspondence and requests for materials should be addressed to Yan Zhou, Liesu Meng or Wenhua Zhu.

Peer review information *Communications Biology* thanks the anonymous reviewers for their contribution to the peer review of this work. Primary Handling Editors: Christopher Larock and Joao Valente.